

Accelerating vapor condensation with daytime radiative cooling

Ming Zhou¹, Haomin Song², Xingyu Xu³, Alireza Shahsafi¹, Zhenyang Xia¹, Zhenqiang Ma¹, Mikhail A. Kats¹, Jia Zhu⁴, Boon S. Ooi⁵, Qiaoqiang Gan^{2, †}, Zongfu Yu^{1, *}

1. Department of Electrical and Computer Engineering, University of Wisconsin – Madison, Madison, WI 53705, USA
2. Department of Electrical Engineering, The State University of New York at Buffalo, Buffalo, NY 14260, USA
3. School of Materials Science and Engineering, Tsinghua University, Beijing 100084, China
4. College of Engineering and Applied Sciences, Nanjing University, Nanjing 210093, China
5. Photonics Laboratory, King Abdullah University of Science and Technology (KAUST), Thuwal, 23955-6900, Saudi Arabia

† Correspondence to: Qiaoqiang Gan (qqgan@buffalo.edu)

* Correspondence to: Zongfu Yu (zyu54@wisc.edu)

Evolution has produced many survival techniques for animals living in extreme arid environments. One of them is the production of water from humid air. Darkling beetles in the Namib desert generate dew from the moisture-rich breeze blown in from the Atlantic. The key to dew generation is the beetle body, which radiatively sheds thermal energy, resulting in cooling that enables the condensation of water. This cooling mechanism has been utilized to develop radiative dew condensers that produce fresh water without consuming energy. However, even the state-of-art radiative dew condenser only works at night and around dawn, before the sun is at full strength, after which the absorption of sunlight swamps the radiative cooling power. Here, we develop daytime radiative condensers that create dew water even in sunlight. We design the thermal radiators to reflect almost all the solar radiation, which has not been previously realized in radiative dew condensers. Compared to state-of-art condensers, our daytime radiative condenser produces double the water over a 24-hour period. The integration of our daytime radiative condenser with solar

water-purification systems can potentially increase water production from 0.4 L m⁻² hour⁻¹ to more than 1 L m⁻² hour⁻¹.

Introduction

Energy and clean water are global challenges that are intertwined in an unfavorable way: even in areas where water is available, energy may not be available to purify water for human use^{1,2}. In this context, there has been strong interest in developing passive clean-water technology that does not actively consume energy. Solar water purification technology is particularly promising because solar energy is abundant and widely accessible. In particular, the solar still, which comprises a solar absorber and a condenser, has a long history³⁻⁷. The solar absorber evaporates the water, which then condenses on the condenser, which dissipates heat into the surrounding environment. Much progress has been made to reduce the cost of solar absorbers⁸ and to improve the evaporation efficiency by localizing heat to nanoscale volumes⁹⁻¹². Sunlight has also been used to harvest atmospheric vapor by evaporating water adsorbed in a porous metal-organic framework¹³.

These solar water-purification technologies involve two energy sources: a heating source for evaporation, and a cooling source for condensation. Most recent works have focused on maximizing the efficiency of sunlight as the heating source⁸⁻¹². The maximum heating power of unconcentrated sunlight is about⁹ 1000 W m⁻², resulting in a maximum evaporation rate of 1.6 L m⁻² hour⁻¹ when assuming that all absorbed solar energy is utilized for evaporation¹⁰. The evaporation efficiency of existing solar evaporation systems is already approaching this theoretical limit. However, there has not been much progress on maximizing condensation efficiency, which ultimately determines the water production rate. Existing solar stills use passive convection and conduction as the cooling sources for condensation¹⁴⁻¹⁷, and the resulting cooling power is much lower than the heating power of sunlight. The difference results in mismatched evaporation and condensation rates, which consequently pins the water production rate to 0.4 L m⁻² hour⁻¹, a quarter of the theoretical limit of evaporation¹⁸.

Radiative cooling can provide an efficient cooling source for condensing vapor. Radiative coolers can operate by dissipating heat into the cold universe via radiative energy transfer, which is made possible by the atmospheric transparency window in mid-infrared (mid-IR) spectral range from 8 to 13 μm . This cooling source is used by darkling beetles in Namib desert to condense water at nighttime¹⁹. The same cooling mechanism has been utilized to develop radiative dew condensers²⁰⁻²². Unfortunately, these radiative condensers are fundamentally incompatible with solar stills since they only work at nighttime. To integrate radiative condenser with a solar still, one needs to maximize its radiation in the mid-IR region and minimize its absorption of sunlight²⁰. However, this goal has never been achieved, as even the best radiative dew condensers absorb more than 16% of sunlight, making them evaporators during the daytime²⁰.

Recently, Fan et al. showed that passive radiative cooling to sub-ambient temperatures can be realized even during the daytime, by integrating a high-efficiency solar reflector and thermal emitter²³. Building upon this work, here we demonstrate a daytime radiative condenser. Compared to traditional passive condensers, our approach offers the following advantages: first, the daytime

radiative condenser provides condensation for vapor at ambient temperature when conduction and convection fail to provide sufficient cooling. Second, compared to existing radiative dew condensers^{20–22}, our condenser can function even in the presence of sunlight, which is essential for integration into solar stills that mainly operate during daytime. Lastly, when used for a component of a solar still, our condenser provides substantial cooling power that can more than double the condensation rate of existing solar stills. The resulting condensation rate can match the evaporation rate to realize efficient phase-change water purification/production systems.

Results

Water vapor condenses when its temperature drops below the dew point, which is lower than the ambient temperature²⁴ when the relative humidity is less than 100%. In such an environment, the only passive cooling mechanism that can enable condensation is thermal radiation, because conduction and convection push the condenser temperature toward the ambient temperature. For example, the black body of the Namib beetles strongly emits infrared radiation around the atmospheric-transparency window¹⁹ (8 ~ 13 μm). Only radiation from the universe emits back to the beetle, but it carries very little thermal energy because of its low average temperature²⁵ of 3 K. Consequently, the Namib beetle can passively dissipate heat through the atmospheric-transparency window to the universe, cooling itself to below the dew point¹⁹.

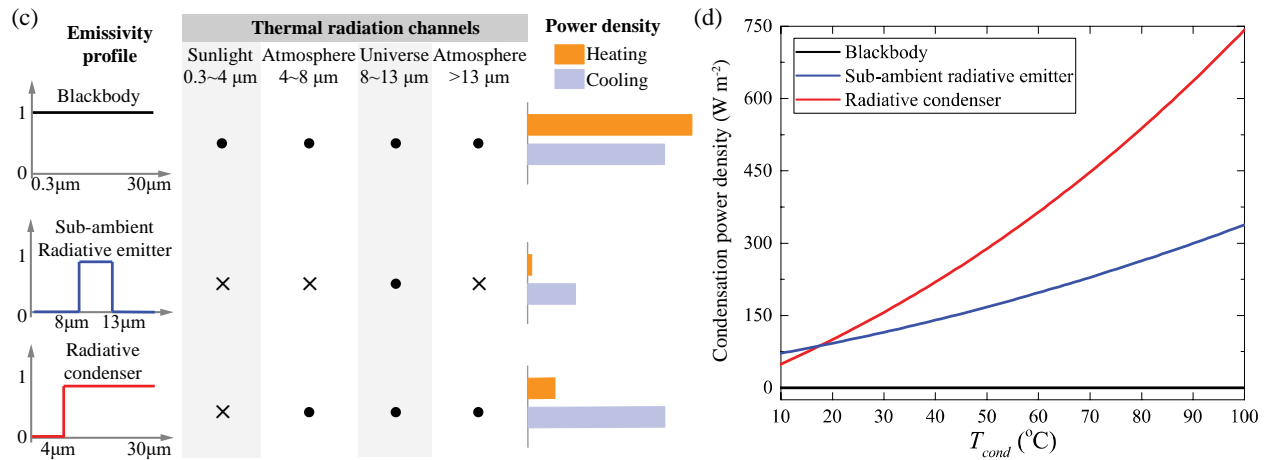
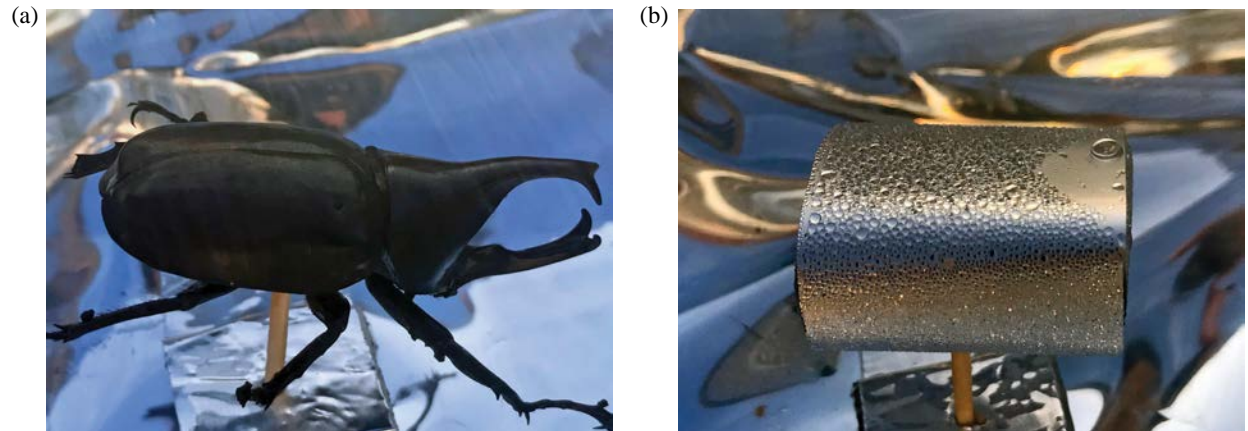


Figure 1. Photos of (a) a black beetle and (b) our artificial daytime-condensing beetle, both placed under sunlight on the roof of a parking ramp of University of Wisconsin - Madison, with 90% ~ 95% humidity air blowing towards them at the same speed. The experiment was performed on April 26th, 2018. The black beetle does not condense vapor due to its absorption of sunlight. In contrast, our artificial beetle reflects most of the sunlight, and thus condenses water vapor during daytime. (c) Thermal radiation channels and emissivity spectra of a blackbody (black), the sub-ambient radiative emitter (blue) from Ref. [23], and our radiative condenser (red). The spectrum of the radiation is divided into four channels - the solar channel (0.3 ~ 4 μm), the universe channel (8 ~ 13 μm) and the two atmospheric channels (4 ~ 8 μm and >13 μm). The dot (cross) indicates that the emitter has the corresponding channel open (closed) for radiative exchange. The heating and cooling power density of the emitters are plotted as orange and blue bars, respectively. (d) Calculated condensation power of the emitters in direct sunlight operating at different vapor temperatures. The ambient temperature is fixed at 20 °C. The blackbody (black) has zero condensation power. The radiative condenser (red) has much more condensation power than the sub-ambient radiative emitter (blue).

Both the Namib beetle and existing radiative dew condensers only work before sun is at full strength. As the sun rises, the heat absorbed by a blackbody due to sunlight radiation can reach¹⁰ 1000 W m⁻², much stronger than the radiation power density of a blackbody at 20 °C, which is around 420 W m⁻². As a result, no condensation can be achieved at daytime. To enable daytime condensation in sunlight, one can spectrally engineer the absorptivity, such the absorption of sunlight in the visible and near-infrared spectral regions is blocked^{20,23,26}. By preventing solar absorption, such a condenser can be made to work during both the day and night. Figure 1 shows a black beetle and an artificial beetle under direct sunlight. The black beetle absorbs most of the sunlight. Our artificial beetle (Fig. 1b) reflects most of the sunlight, but still emits in the mid infrared. When vapor at ambient temperature flows past both “beetles” during daytime, the black beetle does not condense water vapor due to its absorption of sunlight. In contrast, visible water droplets can be seen on our daytime condensing beetle.

Now we explain the design principle of the radiative condenser (“artificial daytime-condensing beetle”). The key is to spectrally engineer the radiative surface to enable or disable specific heat-exchange channels with the environment. The spectrum of the radiation can be roughly divided into four segments under a clear sky during the daytime, as shown in Fig. 1c. In the wavelength range of 0.3 to 4 μm , the incoming radiation is dominated by solar radiation. The heating power density from this channel is calculated as $q_{solar} = \int d\Omega \cos\theta \int_{0.3}^4 d\lambda I_{AM1.5}(\lambda) \epsilon_{cond}(\lambda, \theta)$, where $\epsilon_{cond}(\lambda, \theta)$ is the angle-dependent absorptivity/emissivity of the condenser and $I_{AM1.5}(\lambda)$ is the AM1.5 solar spectral irradiance. From 4 to 8 μm , the incoming radiation is dominated by atmospheric radiation. From 8 to 13 μm , the only incoming radiation is from the universe under clear sky. Beyond 13 μm , the incoming radiation is again dominated by atmospheric radiation. The incoming heating power density in these channels can be calculated as $q_{in} = \int d\Omega \cos\theta \int_{\lambda_1}^{\lambda_2} d\lambda I_{BB}(T_{amb}, \lambda) \epsilon_{atm}(\lambda, \theta)$, where $I_{BB}(T_{amb}, \lambda)$ is the spectral irradiance of a blackbody at ambient temperature T_{amb} . The angle-dependent emissivity of atmosphere is calculated as²⁷ $\epsilon_{atm}(\lambda, \theta) = 1 - t(\lambda)^{1/\cos\theta}$, where $t(\lambda)$ is the atmospheric transmittance in the zenith direction²⁸. Assuming an atmosphere temperature of 20 °C, the heating power density in spectral regions from 4 ~ 8 μm , 8 ~ 13 μm and >13 μm are 50, 40 and 180 W m⁻², respectively.

Meanwhile, the condenser also dissipates heat through radiation in these four channels. The cooling power density radiated by the condenser in these channels can be calculated as $q_{out} =$

$\int d\Omega \cos\theta \int_{\lambda_1}^{\lambda_2} d\lambda I_{BB}(T_{cond}, \lambda) \epsilon_{cond}(\lambda, \theta)$. We developed a steady-state model to calculate the temperature of the condenser T_{cond} under different vapor temperature T_{vapor} (see Supplementary Note 1). The condensation power density then is obtained by subtracting the total heating power density from the total cooling power density.

A blackbody has all four channels open for heat exchange, as shown in Fig. 1c. Thus, the cooling power density reaches 1100 W m^{-2} at $100 \text{ }^\circ\text{C}$. However, the blackbody also receives all the heating power density in the four channels, which reaches 1270 W m^{-2} due to the absorption of solar radiation (1000 W m^{-2}). Thus, a blackbody has no daytime condensation power, even for vapor at $100 \text{ }^\circ\text{C}$ (Fig. 1d). In contrast, Fan et al. designed radiative emitters that close all channels except the universe²⁹ to realize sub-ambient radiative cooling. As a result, the radiative heat received by these radiative emitters is substantially reduced to as low as 40 W m^{-2} , allowing cooling to well below the ambient temperature^{23,25}. However, because the daytime sub-ambient radiative emitter only emits in the spectral region from 8 to $13 \mu\text{m}$, its cooling power is also substantially reduced compared to that of a blackbody, leading to limited condensation power. This design is sub-optimal for a radiative condenser where maximizing condensation power is required. Our radiative condensers only close the solar channel and leave the atmospheric channels completely open, as shown in Fig. 1c. This design is undesirable for sub-ambient cooling³⁰. However, the vapor created by in most solar stills is at or above the ambient temperature, and thus an open atmospheric channel can contribute substantially to condensation. As shown in Fig. 1d, radiative condensers (red line) more than double the cooling power when compared to sub-ambient radiative emitters (blue line) at most vapor temperatures of practical relevance, e.g., in solar stills.

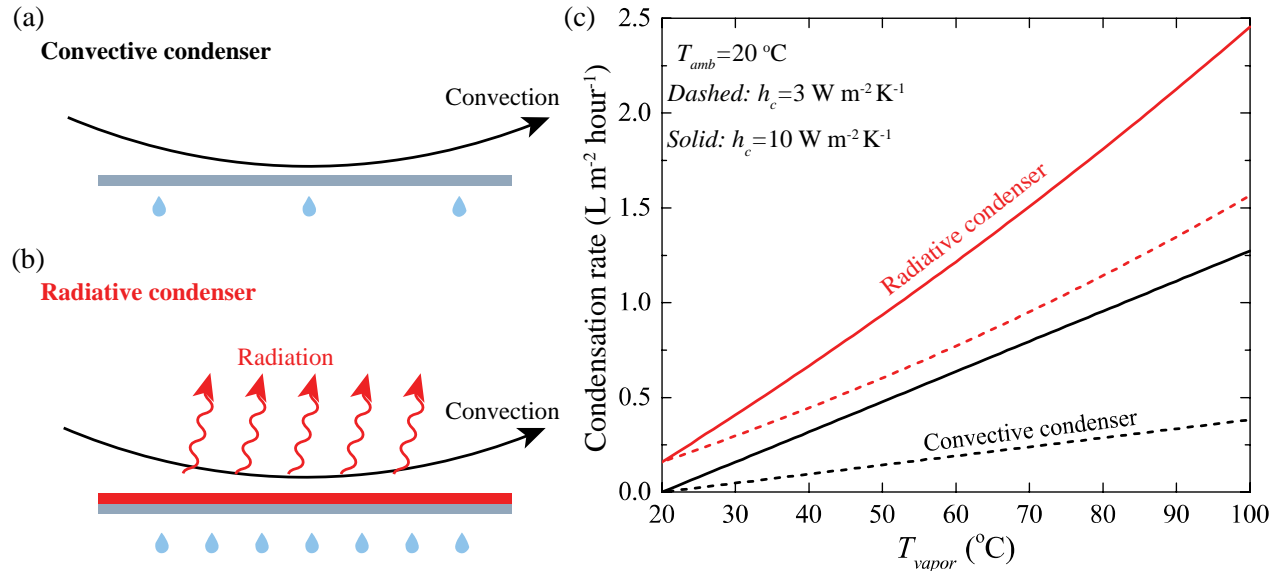


Figure 2. (a) and (b) Schematic of a convective passive condenser (a) and our radiative passive condenser (b). The convective condenser dissipates heat through only convection, while the radiative condenser dissipates heat through both convection and radiation. (c) Theoretically calculated condensation rates of the convective (black) and radiative condenser (red), assuming an ambient temperature of $20 \text{ }^\circ\text{C}$ and relative humidity of 100%.

Next, we discuss the application of our daytime radiative condenser for solar-still systems. The steady-state condensation rates are obtained from our steady-state theoretical model, which is available in Supplementary Note 1.

Water vapor created by sunlight absorption can condense through natural convection (Fig. 2a) because the vapor temperature T_{vapor} in solar stills is above the ambient temperature T_{amb} . The convective cooling power density can be calculated as $P_{conv} \cong h_c(T_{vapor} - T_{amb})$, where h_c is the convective heat transfer coefficient. h_c depends on the wind speed at the surface of the condenser³¹, which usually ranges from 3 to 10 W m⁻² K⁻¹ for wind speed from 0 to 10 mph. The condensation rate W_{water} can be calculated from the cooling power as $W_{water} = P_{conv}/\Delta_{vapor}$, where $\Delta_{vapor} = 2.26 \times 10^6$ J kg⁻¹ is the latent heat from vapor to liquid. Even in the situation most favorable for convective cooling, e.g. vapor at 100 °C and wind speed of 10 mph (black solid curve in Fig. 2b), the condensation rate is only 1.3 L m⁻² hour⁻¹. This rate is below the limit of the one-sun vapor generation rate of 1.6 L m⁻² hour⁻¹¹⁰. The situation becomes much worse when there is no wind (black dashed curve in Fig. 2b). In most practical situations, the vapor temperature is well below 100 °C. For instance, the temperature of water vapor in the solar still in Ref. [8], which was demonstrated to have the highest solar-to-thermal efficiency, is only 40 °C. At such low temperatures, the upper bound of the condensation rate of a convective condenser is less than 0.1 L m⁻² hour⁻¹. This low condensation rate becomes the bottleneck of water production in solar stills. Conversely, the daytime radiative condenser can substantially improve the condensation rate. Even at low temperatures, e.g. 40 °C., the condensation rate without wind is enhanced by more than 4 times, to 0.44 L m⁻²hour⁻¹. At high temperatures, e.g., 100 °C, the condensation rate almost doubles, reaching 2.5 L m⁻² hour⁻¹, well above the theoretical limit of the one-sun evaporation rate. Such a high condensation rate will help to increase vapor-pressure gradient inside a solar still, facilitating the evaporation process.

We now describe the experimental realization of radiative condensers. Figure 3a shows the schematic of a simple, large-area radiator designed to approach the near-ideal condenser absorptivity/emissivity spectrum (black dashed line). It consists of layers of polydimethylsiloxane (PDMS) and silver (Ag) on an aluminum (Al) substrate, with thickness of 100 μm, 150 nm, and 1 mm, respectively. The radiation mainly arises from the PDMS layer, which has a near-unity emissivity for wavelengths longer than 4.5 μm due to Si–O and Si–C bond vibrations³². PDMS is transparent to sunlight, which can be reflected by the Ag layer. The Al substrate is chosen because of its high thermal conductivity. In our experiment, the width and length of the condensation region are 25 cm and 20 cm, respectively. The emissivity of the structure is characterized using Fourier transform infrared (FTIR) spectroscopy and the measured emissivity spectrum is shown in Fig. 3a. Our daytime radiative condenser reflects almost 96% of the solar radiation (0.3~4 μm) and emits efficiently in mid-IR region (>4 μm). We placed the radiator inside an insulating box made from polystyrene, as shown in Fig. 3b. The external surface of the insulating box is covered with aluminum tape to prevent solar heating. A low-density polyethylene film covers the opening of the insulating box to reduce convective heat losses.

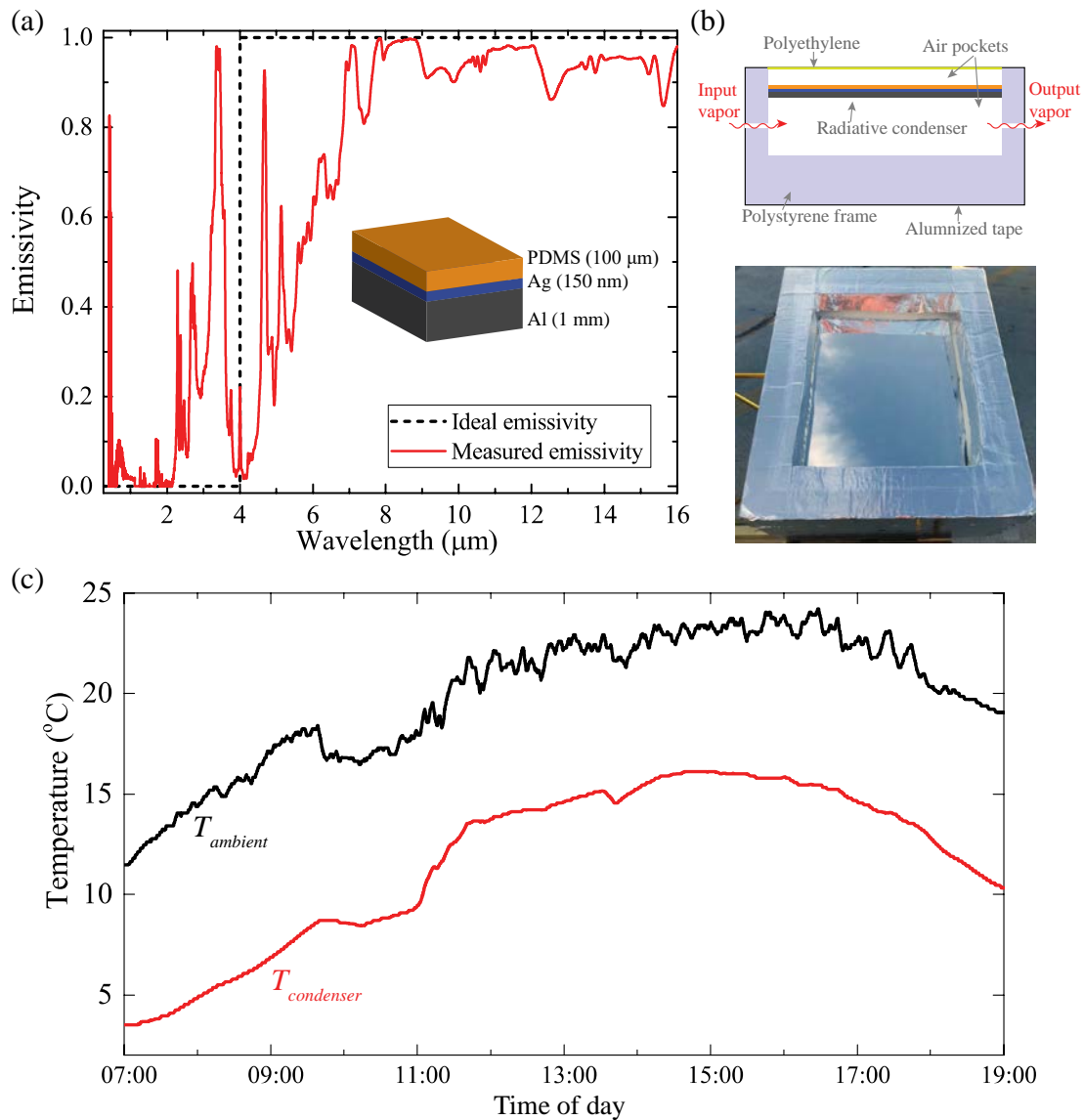


Figure 3. Experimental design of daytime radiative condenser. (a) Schematic of the daytime radiative emitter and measured emissivity spectrum. The emitter consists of a 100- μm layer of PDMS, a 150-nm layer of silver, and a 1-mm-thick aluminum plate. (b) Experimental setup. The emitter is placed inside an insulating polystyrene box. The opening of the insulating box is covered by a thin polyethylene film and the external surface of the box is covered by aluminized foil tape. (c) Temperature under direct sunlight. The temperature of the condenser is about 8 $^{\circ}\text{C}$ lower than the ambient temperature throughout the day. The measurement was performed on the roof of Space Science and Engineering Building of University of Wisconsin – Madison on September 29th, 2017.

To characterize the cooling power of our radiative condenser under direct sunlight, we placed it on a roof facing the sky. The temperature of the condenser is measured by attaching a thermocouple at center of the backside of the condenser with conductive tape. The temperature of the ambient air is measured by placing a thermocouple inside a weather shield to avoid sunlight and wind. The measurement was performed on a sunny day with clear sky from 07:00 to 19:00. Figure 3c shows the temperature of the condenser (red curve) and the ambient air (black curve).

The temperature of the condenser is about 8 °C lower than the ambient temperature throughout the day, which is slightly lower than that of existing sub-ambient radiative emitters³³.

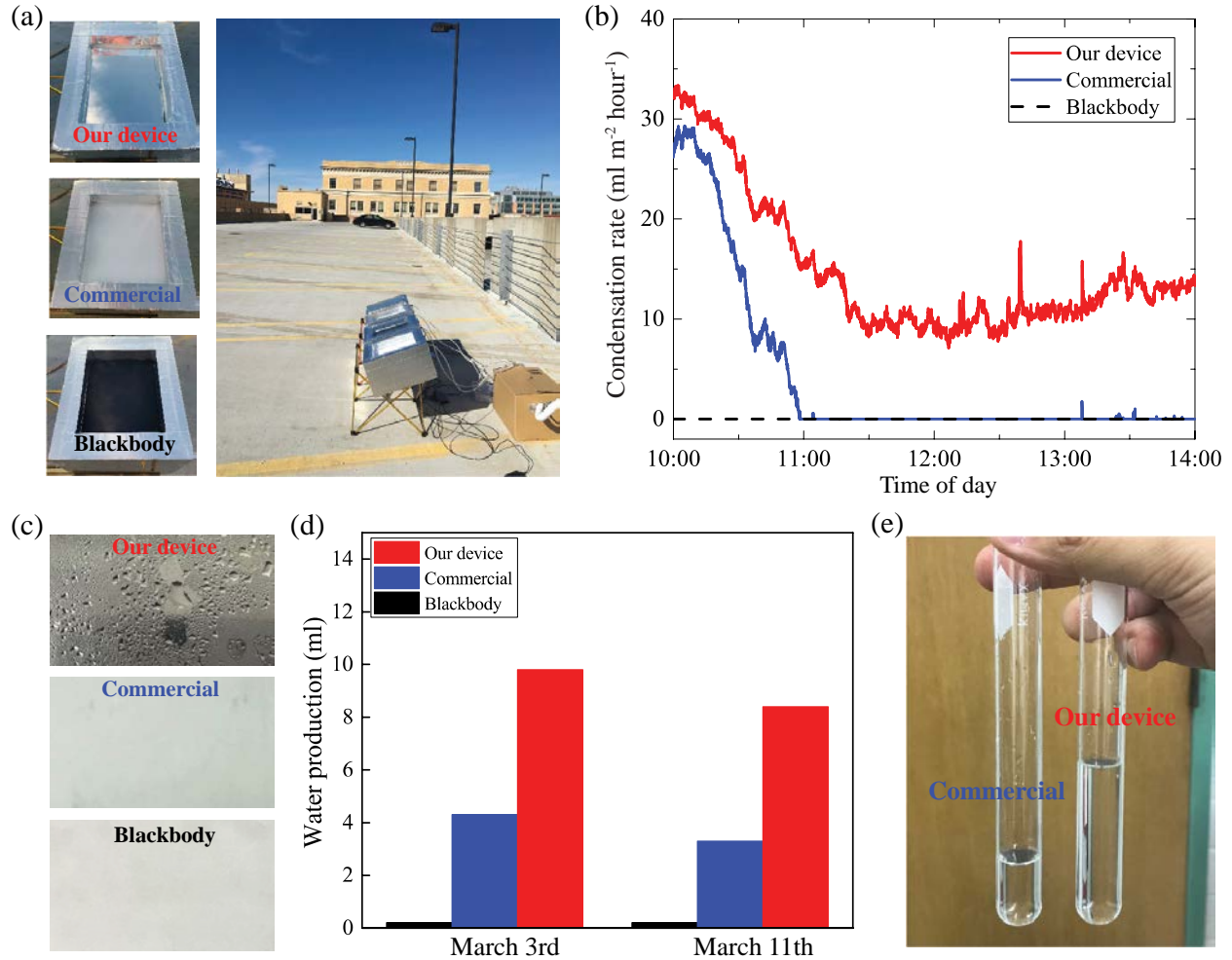


Figure 4. (a) Left: front-side pictures of condensers used in our measurements. A blackbody and a commercial radiative dew condenser, which is known as OPUR foil, are used for comparison. Right: Outdoor experimental setup. The condensers are placed on the roof of a parking ramp of University of Wisconsin - Madison under direct sunlight. (b) Real-time condensation rates of our daytime radiative condenser (red line), a commercial radiative condenser (blue line) and a blackbody radiative condenser (black line). The measurement was performed from March 10th to 11th. For simplicity, we only plot data recorded during daytime on March 10th. The blackbody had zero condensation rate due to absorption of sunlight. The commercial condenser initially had a non-zero condensation rate in the morning, but it dropped to zero around 11:00. Conversely, our daytime condenser remained functional throughout the day. (c) Photos of the condensing surface for each condenser taken around 17:00, March 11th. Visible water droplets can only be seen on our daytime radiative condenser. (d) Daily water productions measured on two different days over more than 24-hour period. (e) A visual comparison between the amount of water produced by our device and the commercial nighttime condenser.

Next, we show daytime condensation for vapor at ambient temperature, such that conduction and convection are completely ineffective.

Two additional condensers were used for comparison: one blackbody emitter and one commercial radiative dew condenser³⁴ as shown in Fig. 4a. The blackbody emitter is made by painting a thick

layer of graphite-based carbon ink on top of an unpolished Al plate, which has the same dimension as our radiative condenser. The commercial condenser is made by a standard material for radiative dew condensation recommended by the International Organization for Dew Utilization (OPUR), which is known as OPUR foil^{26,35}. The OPUR foil consists a white low-density polyethylene foil, with 5% volume of TiO₂ nanoparticles (diameter 0.19 μm) and 5% volume of BaSO₄ nanoparticles (diameter 0.8 μm). It We attached the OPUR foil to an Al plate with the same dimensions as our radiative condenser. In addition to those condensers, a reference device consisting of a plain Al plate was used to measure the ambient temperature and humidity of the input air.

All condensers were placed on a roof facing the sky. Humified air with a relative humidity of 90% ~ 95% was pumped into all condensers at a constant rate of $V_{in} = 0.9 \text{ m}^3 \text{ hour}^{-1}$. The vapor is filtered through a water trap to ensure no water droplets were contained in the vapor entering the cooling chamber. We then performed day-to-night measurements on March 3rd, 10th and 11th of 2018. The temperature T_{out} and relative humidity H_{out} of the output airflow were measured by directly attaching temperature and relative humidity probes at the output outlet. The amount of water contained in the output air flow then was obtained as $m_{out} = H_{out}P(T_{out})V_{in}M_{water}/R$, where $P(T)$ is the vapor pressure at temperature T , R is the ideal gas constant, and M_{water} is the molar mass of water. The vapor pressure $P(T)$ was calculated using the Buck equation³⁶. The condensation rate then was obtained as $W_{cond} = (m_{in} - m_{out})/A_{cond}$, where m_{in} is the amount of water contained in the input air flow and A_{cond} is the area of the condensers. The overall water production of the condensers was obtained by measuring the weight change of the condensers.

Figure 4b shows a typical measurement during daytime. The blackbody absorbs almost all the sunlight and does not condense vapor (black curve). The commercial condenser absorbs less sunlight, and is able to condense vapor in the morning under relatively weak sunlight. Around 11:00, the condensation rate of the commercial condenser (blue curve) also dropped to zero. In contrast, our daytime condenser continued to condense water vapor all day. Figure 4c shows pictures of the back surface of the condensers before sunset. The vapor flows below the condensing surface. Water droplets can be seen on the back surface of our daytime radiative condenser. As shown in Fig. 4d, the daily water production of our daytime radiative condenser is almost twice that of the commercial condenser. On the other hand, the total water production of the blackbody condenser was almost zero because the water condensed at night is evaporated during daytime. Note it's difficult to collect the produced water from our condensers due to the small condensing area (0.05 m²).

A radiative condenser can also be designed to be transparent to solar radiation, and still be highly emissive in the infrared. Such a radiative condenser provides similar condensation performance as the device in Fig. 3 and 4, and can be directly integrated with existing solar stills. An example of transparent radiative condenser is given in Supplementary Note 2.

In conclusion, we demonstrate a passive device—a daytime radiative condenser—that can significantly accelerate the condensation of vapor. We experimentally demonstrated water condensation of ambient-temperature vapor under direct sunlight, which cannot be realized by either conventional radiative condensers or convective condensers. By extending the operation to daytime, the radiative condenser can be incorporated into solar water-purification technologies, in

which the cc power is generally lower than the solar heating power, creating the imbalance of evaporation and condensation rates. Daytime radiative condensers can remove this imbalance, increasing total water production by roughly a factor of two.

Acknowledgements: M. K. acknowledges support from the National Science Foundation (ECCS-1750341). Z. Y. and M. Z. acknowledges support from the National Science Foundation (CMMI-156197). M. Z. acknowledges support from the 3M fellowship.

References

1. Shannon, M. A. *et al.* Science and technology for water purification in the coming decades. *Nature* **452**, 301–310 (2008).
2. Elimelech, M. & Phillip, W. A. The Future of Seawater Desalination: Energy, Technology, and the Environment. *Science* **333**, 712–717 (2011).
3. Sodha, M. S., Kumar, A., Tiwari, G. N. & Tyagi, R. C. Simple multiple wick solar still: Analysis and performance. *Solar Energy* **26**, 127–131 (1981).
4. Malik, M. A. S. *Solar distillation: a practical study of a wide range of stills and their optimum design, construction, and performance.* (Pergamon, 1982).
5. Fath, H. E. S. Solar distillation: a promising alternative for water provision with free energy, simple technology and a clean environment. *Desalination* **116**, 45–56 (1998).
6. Kalogirou, S. A. Seawater desalination using renewable energy sources. *Progress in Energy and Combustion Science* **31**, 242–281 (2005).
7. Ali Samee, M., Mirza, U. K., Majeed, T. & Ahmad, N. Design and performance of a simple single basin solar still. *Renewable and Sustainable Energy Reviews* **11**, 543–549 (2007).
8. Liu, Z. *et al.* Extremely Cost-Effective and Efficient Solar Vapor Generation under Nonconcentrated Illumination Using Thermally Isolated Black Paper. *Global Challenges* **1**, 1600003 (2017).

9. Ghasemi, H. *et al.* Solar steam generation by heat localization. *Nature Communications* **5**, 4449 (2014).
10. Ni, G. *et al.* Steam generation under one sun enabled by a floating structure with thermal concentration. *Nature Energy* **1**, 16126 (2016).
11. Zhou, L. *et al.* 3D self-assembly of aluminium nanoparticles for plasmon-enhanced solar desalination. *Nature Photonics* **10**, 393–398 (2016).
12. Zhao, F. *et al.* Highly efficient solar vapour generation via hierarchically nanostructured gels. *Nature Nanotechnology* **1** (2018). doi:10.1038/s41565-018-0097-z
13. Kim, H. *et al.* Water harvesting from air with metal-organic frameworks powered by natural sunlight. *Science* eaam8743 (2017). doi:10.1126/science.aam8743
14. Dimri, V., Sarkar, B., Singh, U. & Tiwari, G. N. Effect of condensing cover material on yield of an active solar still: an experimental validation. *Desalination* **227**, 178–189 (2008).
15. El-Sebaili, A. A. Effect of wind speed on active and passive solar stills. *Energy Conversion and Management* **45**, 1187–1204 (2004).
16. El-Sebaili, A. A. On effect of wind speed on passive solar still performance based on inner/outer surface temperatures of the glass cover. *Energy* **36**, 4943–4949 (2011).
17. Vinoth Kumar, K. & Kasturi Bai, R. Performance study on solar still with enhanced condensation. *Desalination* **230**, 51–61 (2008).
18. Gupta, D. B. & Mandraha, T. K. Thermal Modeling and Efficiency of Solar Water Distillation: A Review. *American Journal of Engineering Research* **11** (2013).
19. Guadarrama-Cetina, J. *et al.* Dew condensation on desert beetle skin. *Eur. Phys. J. E* **37**, 109 (2014).

20. Nilsson, T. M. J., Vargas, W. E., Niklasson, G. A. & Granqvist, C. G. Condensation of water by radiative cooling. *Renewable Energy* **5**, 310–317 (1994).
21. Muselli, M. *et al.* Dew water collector for potable water in Ajaccio (Corsica Island, France). *Atmospheric Research* **64**, 297–312 (2002).
22. Maestre-Valero, J. F., Martínez-Alvarez, V., Baille, A., Martín-Górriz, B. & Gallego-Elvira, B. Comparative analysis of two polyethylene foil materials for dew harvesting in a semi-arid climate. *Journal of Hydrology* **410**, 84–91 (2011).
23. Raman, A. P., Anoma, M. A., Zhu, L., Rephaeli, E. & Fan, S. Passive radiative cooling below ambient air temperature under direct sunlight. *Nature* **515**, 540–544 (2014).
24. Lawrence, M. G. The Relationship between Relative Humidity and the Dewpoint Temperature in Moist Air: A Simple Conversion and Applications. *Bull. Amer. Meteor. Soc.* **86**, 225–234 (2005).
25. Chen, Z., Zhu, L., Raman, A. & Fan, S. Radiative cooling to deep sub-freezing temperatures through a 24-h day–night cycle. *Nature Communications* **7**, 13729 (2016).
26. Khalil, B. *et al.* A review: dew water collection from radiative passive collectors to recent developments of active collectors. *Sustain. Water Resour. Manag.* **2**, 71–86 (2016).
27. Granqvist, C. G. & Hjortsberg, A. Radiative cooling to low temperatures: General considerations and application to selectively emitting SiO films. *Journal of Applied Physics* **52**, 4205–4220 (1981).
28. Lord, S. D. *A new software tool for computing Earth's atmospheric transmission of near- and far-infrared radiation.* (1992).
29. Rephaeli, E., Raman, A. & Fan, S. Ultrabroadband Photonic Structures To Achieve High-Performance Daytime Radiative Cooling. *Nano Lett.* **13**, 1457–1461 (2013).

30. Kou, J., Jurado, Z., Chen, Z., Fan, S. & Minnich, A. J. Daytime Radiative Cooling Using Near-Black Infrared Emitters. *ACS Photonics* **4**, 626–630 (2017).
31. Watmuff, J. H., Charters, W. W. S. & Proctor, D. *Solar and wind induced external coefficients - Solar collectors*. 56 (1977).
32. Cai, D. K., Neyer, A., Kuckuk, R. & Heise, H. M. Optical absorption in transparent PDMS materials applied for multimode waveguides fabrication. *Optical Materials* **30**, 1157–1161 (2008).
33. Zhai, Y. *et al.* Scalable-manufactured randomized glass-polymer hybrid metamaterial for daytime radiative cooling. *Science* eaai7899 (2017). doi:10.1126/science.aai7899
34. Nilsson, T. M. J. & Niklasson, G. A. Radiative cooling during the day: simulations and experiments on pigmented polyethylene cover foils. *Solar Energy Materials and Solar Cells* **37**, 93–118 (1995).
35. International Organization For Dew Utilization. Available at: <http://www.opur.fr/>. (Accessed: 27th April 2018)
36. Buck, A. L. New Equations for Computing Vapor Pressure and Enhancement Factor. *J. Appl. Meteor.* **20**, 1527–1532 (1981).

Supplementary Information

Supplementary Note 1. Steady-state model of passive condensation systems

We developed a steady-state model to calculate the condensation rate of passive condensation systems. Below we describe it in detail.

As we discussed in the manuscript, the major cooling sources in passive condensers that operate without additional energy input are convection and radiation. The cooling power from conduction is generally small comparing to that from convection and is not considered here. The convective cooling power density q_{conv} and radiative cooling power density q_{rad} are given by

$$q_{conv}(T_{cond}) = h_c(T_{cond} - T_{amb}) \quad (1)$$

$$q_{rad}(T_{cond}) = \int d\Omega \cos\theta \int_0^{+\infty} d\lambda I_{BB}(T_{cond}, \lambda) \epsilon_{cond}(\lambda, \theta) \quad (2)$$

Here h_c is the convective heat transfer coefficient, T_{cond} and T_{amb} are the temperature of the condenser and the surrounding environment, respectively. $I_{BB}(T, \lambda)$ is the spectral intensity of a blackbody at temperature T . $\epsilon_{cond}(\lambda, \theta)$ is the spectral emissivity of the condenser.

The major heating sources are the solar radiation and atmospheric radiation, whose heating power density are given by

$$q_{solar} = \int d\Omega \cos\theta \int_0^{+\infty} d\lambda I_{AM1.5}(\lambda) \epsilon_{cond}(\lambda, \theta) \quad (3)$$

$$q_{atm} = \int d\Omega \cos\theta \int_0^{+\infty} d\lambda I_{BB}(T_{atm}, \lambda) \epsilon_{cond}(\lambda, \theta) \epsilon_{atm}(\lambda, \theta) \quad (4)$$

Here $I_{AM1.5}(\lambda)$ is the AM1.5 solar spectral irradiance and T_{atm} is the atmosphere temperature. For a clear sky, T_{atm} is the same as or lower than the ambient temperature T_{amb} . Here for simplicity, we assume the $T_{atm} = T_{amb}$ throughout our calculation. The angle-dependent emissivity of the atmosphere is given by¹ $\epsilon_{atm}(\lambda, \theta) = 1 - t(\lambda)^{1/\cos\theta}$, where $t(\lambda)$ is the atmospheric transmittance in the zenith direction².

As humidified air with temperature T_{input} and relative humidity $H_{relative}$ flows through the condenser, it is cooled down to the temperature of the condenser T_{cond} . The required cooling power density is given by

$$q_{air}(T_{cond}) = C_{V,air} u (T_{cond} - T_{in}) \quad (5)$$

Here $C_{V,air}$ is the specific heat capacity of air at constant volume u is the speed of the input air flow at the air-condenser interface.

The vapor pressure decreases as the temperature is cooled down. Condensation occurs when the vapor pressure reaches the saturation vapor pressure. We approximated the saturation vapor pressure $P(T)$ at temperature T using the Buck equation³:

$$P(T) = 611.21 \exp\left(\left(18.678 - \frac{T - 273.15}{234.5}\right)\left(\frac{T - 273.15}{T - 16.01}\right)\right) \quad (6)$$

The amount of cooling power density required for condensation of vapor is given by

$$q_{vapor}(T_{cond}) = u\Delta_{vap} \left(\frac{H_{relative}P(T_{in})}{RT_{in}} - \frac{P(T_{cond})}{RT_{cond}} \right) \quad (7)$$

where R is the ideal gas constant. The latent heat from vapor to liquid water is given by $\Delta_{vap} = 40.63$ kJ/mol.

At steady state, the whole system reaches thermal equilibrium, which satisfies

$$q_{conv}(T_{cond}) + q_{rad}(T_{cond}) - q_{solar} - q_{atm} = q_{vapor}(T_{cond}) + q_{air}(T_{cond}) \quad (8)$$

By solving Eq. 8, we obtain the working temperature of the condenser T_{cond} , which depends on the input humidity $H_{relative}$ and air flow rate u . The condensation rate of the condenser then can be calculated as

$$W_{water} = \frac{q_{vapor}}{\Delta_{vap}} M_{water} \quad (9)$$

where M_{water} is the molar mass of water.

To validate our theoretical model, we predict the condensation rate of our condenser based on measured T_{in} , T_{amb} and H_{in} , and compare it to the measurement. The measurement was performed from March 10th to 11th on the roof a parking ramp of University of Wisconsin – Madison. The input air flow rate $u = 0.025$ m/s. The convective heat transfer coefficient h_{conv} is taken to be $6 \text{ Wm}^{-2}\text{K}^{-1}$ to fit the experimental data. The results are plotted in Fig. S1. The predicted condensation rate (red curve) fits the measurement (black curve) very well. Here for simplicity, we consider nighttime condensation where the solar radiation is completely suppressed, i.e. $q_{solar} = 0$.

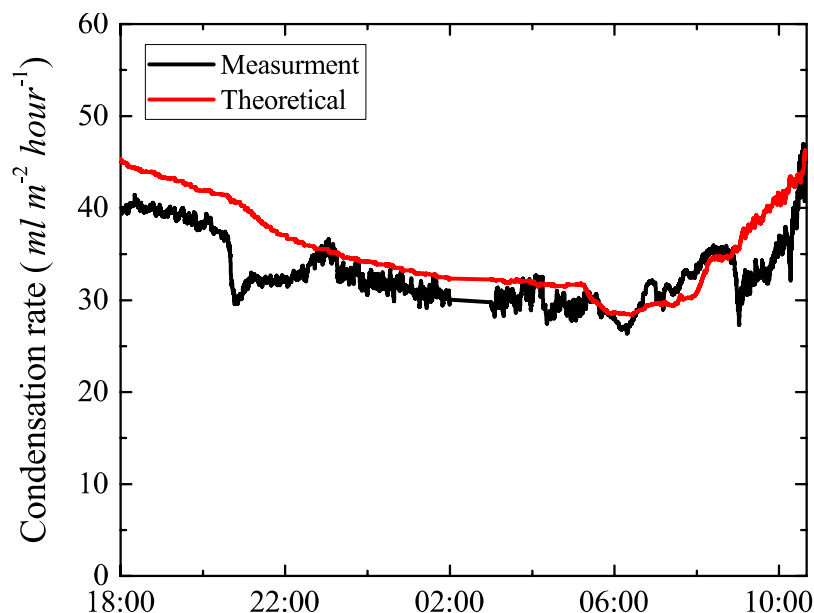


Figure S1. The theoretically predicated nighttime condensation rate (red) fits the experimental measurements (black) very well.

Supplementary Note 2. Transparent daytime radiative condenser

Here we propose a simple design of a transparent daytime radiative condenser that can be readily implemented in existing solar stills. As shown in Fig. S2a, the transparent radiative condenser consists of a thin layer of PDMS, which has a thickness of 100 μm , on top of glass. Figure S2b shows the transmission (red curve) and emissivity (black curve) spectra of the PDMS-glass condenser, which is more than 93% transparent to solar radiation. The structure also has near-unity emissivity in the mid-IR region. As a result, it has similar radiative condensing performance as the daytime radiative condenser described in Fig. 4 in the manuscript.

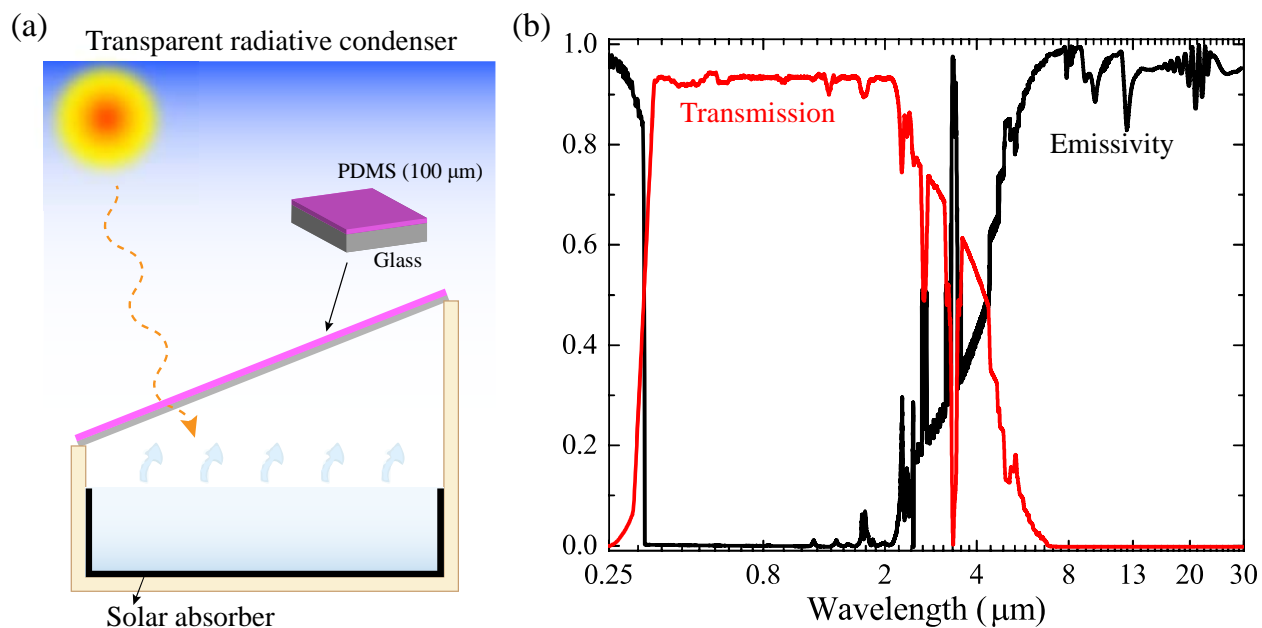


Figure S2. Transparent radiative condenser. (a) The transparent condenser can be readily implemented in existing solar stills. The structure is a layer of PDMS with a thickness of 100 μm on top of a glass substrate. (b) Transmission (red) and emissivity (black) spectra.

References

1. Granqvist, C. G. & Hjortsberg, A. Radiative cooling to low temperatures: General considerations and application to selectively emitting SiO films. *Journal of Applied Physics* **52**, 4205–4220 (1981).
2. Lord, S. D. *A new software tool for computing Earth's atmospheric transmission of near- and far-infrared radiation*. (1992).
3. Buck, A. L. New Equations for Computing Vapor Pressure and Enhancement Factor. *J. Appl. Meteor.* **20**, 1527–1532 (1981).